Improvement of Sensorless Control Performance in Low Speed Area Based on FFT Analysis

Jaemin Lee, Wahyu Kunto Wibowo, and Seokkwon Jeong

Abstract— This paper investigates improvement of sensorless speed control in low speed area for permanent magnet synchronous motors (PMSMs) based on an adaptive sliding mode observer (SMO) for electric propulsion system of small ships. An adaptive gain, cascade low pass filter (LPF), and phase delay compensation are utilized in the conventional SMO for reducing inherent chattering phenomenon. Those solutions are designed in the way of adaptive type connected with rotor speed. The experimental results from a 1.5 kW PMSM are provided to verify the effectiveness of the proposed SMO. The fast Fourier transform (FFT) analysis is performed to reveal and clarify the effectiveness of the proposed SMO. The result shows that the proposed SMO gives fairly good speed control performance without a sensor even when the PMSM operates at 0.005 p.u.

Index Terms— Sensorless speed control, Permanent magnet synchronous motor, Adaptive sliding mode observer, Cascade low-pass filter, Fast Fourier transform, Electric propulsion system

I. Introduction

Recently, electric propulsion system (EPS) has been focused on the marine industrial field as the main thruster of ships. The EPS becomes a high candidate of technology to replace the conventional propulsion system, propeller system, due to environmental emission reduction, low vibration, and compactness of the system [1]. Nowadays, a permanent magnet synchronous motor (PMSM) receives high attention in all industrial fields, especially for adjustable speed and position applications.

The PMSM has the ability to produce constant torque, high power density, fast dynamics, high efficiency, and rugged structure [2]. All of those advantages are suitable as the prime mover in the EPS. In the speed control of a PMSM, it requires the information of the rotor speed and rotor angular position. Usually, a physical sensor such as resolvers and encoders is used to obtain the rotor angular position [3]. However, the motors of the ship propulsion system are located in a harsh environment due to severe moisture, humidity, and vibration. The physical sensors often cannot be accommodated in those conditions because of reliability concern and physical constraints. Hence, sensorless control technique without physical sensors of the PMSMs is applied to the EPS for the small ships.

In this paper, a new strategy to improve the performance of sensorless control based on the conventional SMO in low speed area for a PMSM is investigated for the EPS of small ships. SMO is widely used to estimate speed and rotor position precisely from back electromotive force (EMF) in the PMSMs due to their strong robustness against motor parameters and noises. However intrinsic chattering phenomenon happens because the conventional SMO is based on a discontinuous switching function such as signum function. The chattering is a main cause of deterioration of the sensorless control performance especially in the low speed area. In order to reduce the chattering problem and to improve the estimation of rotor speed and angular position, this paper proposes the utilization of SMO that has a speed-adaptive observer gain and a cascade LPF with variable cut-off frequency. Also, phase delay compensation is used to reduce phase delay cause by the cascade LPF. The method of fast Fourier transform (FFT) analysis is performed to reveal and clarify the effectiveness of the proposed SMO.

The proposed strategy is applied to a 32-bit fixed digital signal processor and 1.5 kW PMSM. Several experiments are conducted to verify the validity of the proposed SMO by the test system. The experimental results show that the proposed method gives fairly good speed control performance and strong robustness even when the PMSM operates at 0.5% from its rated speed value.

II. Mathematical Model of The PMSM Based on The SMO for Speed and Rotor Position Sensorless

The current model of the surface mounted PMSM in an αβ stationary reference frame is shown as follows:

$$\begin{bmatrix} pi_\alpha \\ pi_\beta \end{bmatrix} = -\frac{R_s}{L_s}\begin{bmatrix} i_\alpha \\ i_\beta \end{bmatrix} + \frac{1}{L_s}\begin{bmatrix} v_\alpha \\ v_\beta \end{bmatrix} - \frac{1}{L_s}\begin{bmatrix} e_\alpha \\ e_\beta \end{bmatrix} \quad (1)$$

$$\begin{bmatrix} e_\alpha \\ e_\beta \end{bmatrix} = \omega_r \psi_r \begin{bmatrix} -\sin\theta_r \\ \cos\theta_r \end{bmatrix} \quad (2)$$

where $v_\alpha, v_\beta, i_\alpha$, and i_β are the stator voltages and currents in the stationary reference frame. R_s and L_s are the stator resistance and inductance respectively. ω_r and ψ_r represent the electrical rotor angular speed and flux linkage generated by the rotor magnet. Notation p is the derivative of time operation. e_α and e_β are back-EMF in an αβ stationary reference frame. Symbol θ_r represents the position of the rotor flux.

The SMO is applied to the system as a replacement for the

Manuscript received April 5, 2017. This work was supported by the Technological Innovation R&D Program (C0406573) funded by the Small and Medium Business Administration(SMBA, Korea)

Jaemin Lee is with Department of Interdisciplinary of Mechatronics Engineering, Pukyong National University (PKNU) Busan, 48547, Korea (e-mail: mywoals125@ naver.com).

Wahyu Kunto Wibowo is with Department of Electrical Engineering, Universitas Pertamina, Jakarta, Indonesia (e-mail: wahyukuntowibowo@gmail.com).

Seokkwon Jeong is coauthor with Department of Refrigeration and Air Conditioning Engineering, PKNU, Busan, 48547, Korea (e-mail: skjeong@pknu.ac.kr).

physical sensor to obtain the information of the speed and rotor position of the PMSM. Eq. (1) is directly used to design the current observer as shown in Eq. (3).

$$\begin{bmatrix} p\hat{i}_\alpha \\ p\hat{i}_\beta \end{bmatrix} = -\frac{R_s}{L_s}\begin{bmatrix} \hat{i}_\alpha \\ \hat{i}_\beta \end{bmatrix} + \frac{1}{L_s}\begin{bmatrix} v_\alpha \\ v_\beta \end{bmatrix} - \frac{1}{L_s}\begin{bmatrix} z_\alpha \\ z_\beta \end{bmatrix} \tag{3}$$

$$\begin{bmatrix} z_\alpha \\ z_\beta \end{bmatrix} = K\begin{bmatrix} \mathrm{sgn}(\hat{i}_\alpha - i_\alpha) \\ \mathrm{sgn}(\hat{i}_\beta - i_\beta) \end{bmatrix} \tag{4}$$

Where the symbol hat "^" denotes the estimated value. The K is the constant observer gain and symbol z is the switching signal which contains the estimated back-EMF information. Dynamic estimation error can be obtained by subtracting Eq. (1) from Eq. (3):

$$\begin{bmatrix} p\bar{i}_\alpha \\ p\bar{i}_\beta \end{bmatrix} = -\frac{R_s}{L_s}\begin{bmatrix} \bar{i}_\alpha \\ \bar{i}_\beta \end{bmatrix} + \frac{1}{L_s}\begin{bmatrix} e_\alpha \\ e_\beta \end{bmatrix} - \frac{1}{L_s}\begin{bmatrix} z_\alpha \\ z_\beta \end{bmatrix} \tag{5}$$

where the symbol bar, "-", represents estimation error of each corresponding variable. The sliding surface is selected as:

$$S = \begin{bmatrix} i_\alpha \\ i_\beta \end{bmatrix} - \begin{bmatrix} \hat{i}_\alpha \\ \hat{i}_\beta \end{bmatrix} \tag{6}$$

When the estimated current reaches the sliding surface, then the estimation error becomes zero and the estimated current tracks the actual value. Hence, $\hat{i}_s = i_s$, Eq. (6) will give:

$$\begin{bmatrix} e_\alpha \\ e_\beta \end{bmatrix} = K\,\mathrm{sgn}\begin{bmatrix} \bar{i}_\alpha \\ \bar{i}_\beta \end{bmatrix} \tag{7}$$

The signum function was used in the conventional SMO as shown in Eq. (7). The usage of this function induces chattering problem. First order LPF is taking a place in the algorithm to minimize the chattering problem as represented in Eq. (8).

$$\begin{bmatrix} \hat{e}_\alpha \\ \hat{e}_\beta \end{bmatrix} = \frac{\omega_c}{s+\omega_c}\begin{bmatrix} z_\alpha \\ z_\beta \end{bmatrix} \tag{8}$$

Where ω_c is the angular speed of the LPF which contains cut-off frequency f_c. The estimated back-EMF results are directly used to calculate the rotor flux position and speed estimation as described in Eq. (9) and Eq. (10).

$$\theta_r = -\tan^{-1}\frac{\hat{e}_\alpha}{\hat{e}_\beta} \tag{9}$$

$$\omega_r = \frac{d\theta_r}{dt} \tag{10}$$

III. Reduction of The Chattering Phenomenon

In this paper, an adaptive speed-observer gain is used to overcome the problem of constant gain observer on the SMO. The adaptive observer gain is designed through the Lyapunov stability criterion. The Lyapunov function candidate is defined in Eq. (11) to design the adaptive observer gain and to set up the stability condition of the SMO.

$$V = \frac{1}{2}S^T S = \frac{1}{2}\hat{i}_\alpha^{\,2} + \hat{i}_\beta^{\,2} \tag{11}$$

The Lyapunov stability condition is satisfied with $K > \max(|e_\alpha|, |e_\beta|)$. The K is used in the conventional SMO as a constant value. The back-EMF, which described in Eq. (2), will reach the maximum value when the values of $\sin\theta_r$ and $\cos\theta_r$ are equal to 1. Hence, the adaptive observer gain of Eq. (12) can be obtained. In the proposed SMO, the cascade LPF was applied to eliminate harmonics caused by chattering and the phase delay compensation shown in Eq. (13) is incorporated.

$$K = \omega_r^* \psi_r \tag{12}$$

$$\Delta\theta = \tan^{-1}\frac{2\omega_r\omega_c}{\omega_c^{\,2} - \omega_r^{\,2}} \tag{13}$$

Where ω_r^* means speed reference. The adaptive observer gain can adjust the actual back-EMF so that the gain is enough to estimate the back-EMF precisely and able to suppress the chattering problem.

A second order cascade LPF with variable cut-off frequency is applied to the proposed SMO. The cut-off frequency of the LPF, $f_c = nP/120$, and its phase delay are varied based on the given speed reference *n*. The P means pole number. The saturation function is needed instead of the signum function to reduce chattering. Also phase delay compensation is designed to promote speed estimation performance.

Fig. 1 shows the block diagram of the proposed SMO included suggested solutions in this paper.

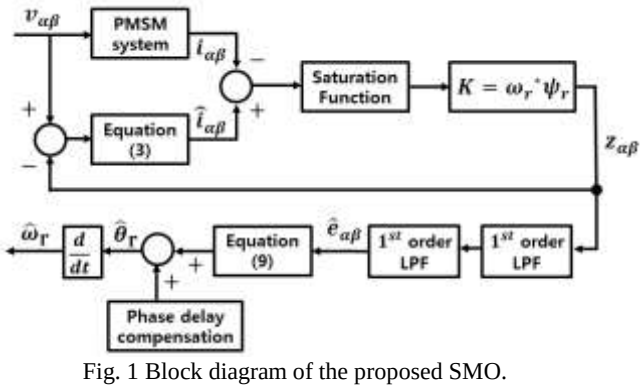

Fig. 1 Block diagram of the proposed SMO.

IV. Experimental Results and FFT Analysis

The experimental setup is shown in Fig. 2 and motor parameters are shown in Table I. The sampling period of the control system was set as 100 μs. In this experiment, the proposed SMO as shown in Fig. 1 was examined to check the effectiveness of the proposed method.

Fig. 2 The experimental system.

TABLE I: PARAMETERS OF THE TESTED PMSM

Parameter (symbol)	Value (unit)
Rated power(P_r)	1.5 (kW)
Rated torque(T_e)	7.16 ($N \cdot m$)
Rated speed(n)	2000 (rpm)
Stator resistance(R_s)	0.4 (Ω)
Stator inductance(L_s)	4.9×10^{-3}(H)
Flux linkage(ψ_r)	0.145 (Wb)
Inertia(J)	1.45×10^{-3}(kg·m^2)
Pole number(P)	8

A. *The conventional SMO*

In this experiment, the conventional SMO with a signum as a switching function was used to estimate speed and position. The speed reference profile was firstly set at 1,000 rpm, then decreases into 500 rpm, and finally changed to 40 rpm. The observer gain K and the cut-off frequency f_c of the first-order LPF were set as a constant value based on the maximum rated speed of the motor. Phase delay compensation is not conducted.

Fig. 3 shows speed, rotor flux position, and back-EMF estimation obtained from experimental result of the PMSM by the conventional SMO.

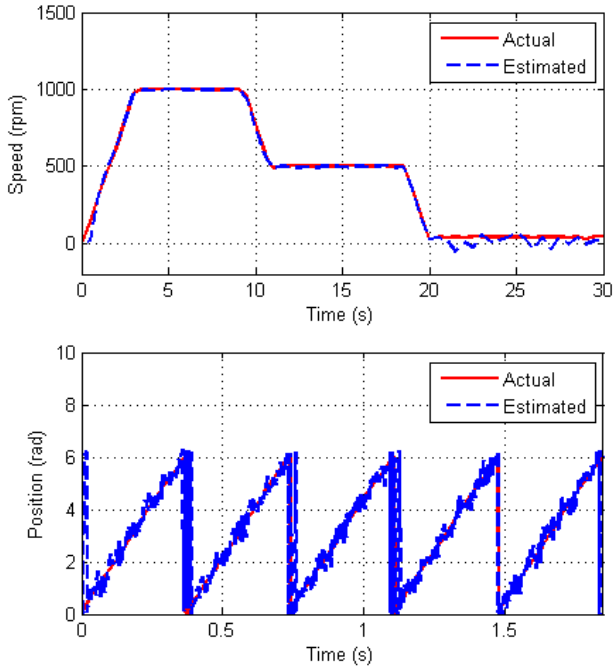

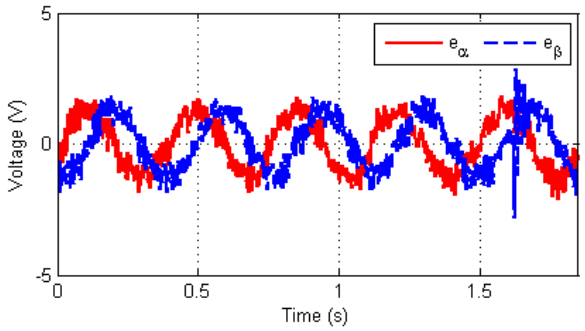

Fig. 3 Experimental result of estimation performance of the PMSM by the conventional SMO at 40rpm ($K=104$, $f_c=133.33Hz$). (From top to the bottom: speed response, rotor flux position, back-EMF estimation)

From the speed and position response shown in Fig. 3, the estimation results suffer from the chattering problem in low speed range. The usage of a signum as the discontinuous function in the conventional SMO becomes the main cause of the chattering appearance on the estimation result. The back-EMF in Fig. 3 has the chattering problem because of the utilization of the signum function even though the first-order LPF is used. It is noted here that the first-order LPF was failed to decrease the chattering problem because of the chattering mostly appeared in lower frequency than the pre-set cut-off frequency of the first-order LPF. Based on Fig. 3, this is why the conventional SMO was only preferred for the medium to high-speed operation range. This result means that the conventional SMO is not suitable for the low-speed estimation.

Fig. 4 shows the FFT analysis result on the back-EMF shown in the Fig. 3 by the conventional SMO.

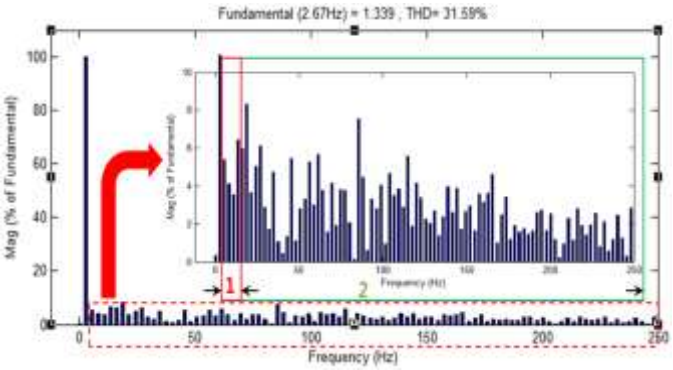

Fig. 4 FFT analysis on the back-EMF estimation result by the conventional SMO at 40 rpm.

The total harmonics distortion (THD) explains the harmonics distortion caused by the chattering problem that affects the back-EMF estimation. The harmonics in the back-EMF were come from several reasons, such as the usage of the switching device, non-linear loads, electrical components, and noises from the power source. Based on Fig. 4, the THD result from the FFT analysis was 31.59%. The harmonics that happened in the back-EMF represent the chattering problem in the conventional SMO. It was assumed that the harmonics in the region 1 in Fig. 4 is mainly caused by the signum function in the SMO. The use of a signum function and constant observer gain needs to be replaced by other

https://doi.org/10.17758/EAP.EAP517021

methods. Also, the first-order LPF was not enough to suppress the chattering problem of the conventional SMO in this speed area. A stronger filter is needed to suppress the chattering problem.

B. The SMO by using the saturation function

In this experiment, the signum function in the conventional SMO was replaced by the saturation function as a switching function. The observer gain K and the cut-off frequency f_c of the first order LPF were set as a constant value. Phase delay compensation is not conducted.

Fig. 5 shows experimental result on the back-EMF estimation of the PMSM by using the SMO with saturation function at 40 rpm and its FFT analysis.

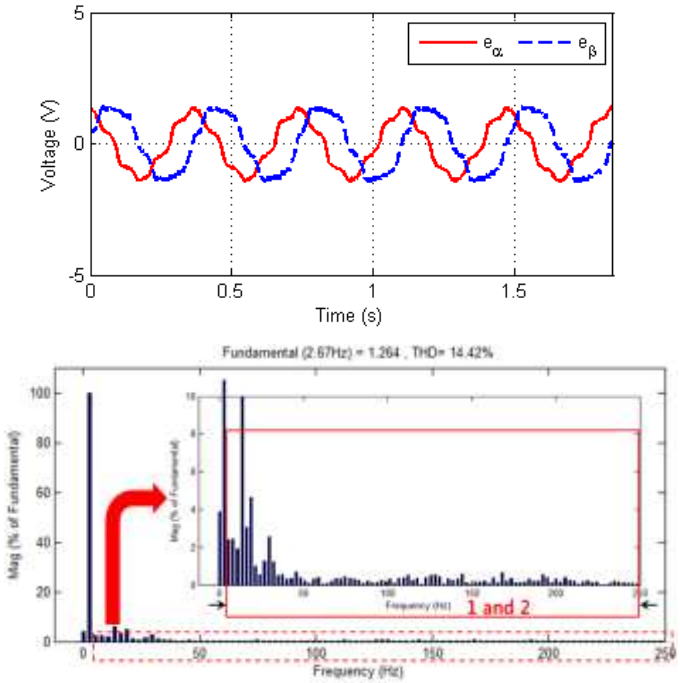

Fig. 5 Experimental result of back-EMF by using the SMO with the saturation at 40 rpm and FFT analysis ($K = 104$, $f_c = 133.33Hz$) . (From top to the bottom: back-EMF estimation, FFT analysis on the back-EMF)

From FFT analysis on the back-EMF shown in Fig. 5, the THD result was 14.42%. The saturation function significantly decreases the chattering. However, the result is not enough to establish good estimation of back-EMF in low speed area. This means that another solution to suppress the chattering should be considered.

C. The SMO by using saturation function and an speed adaptive observer gain

In this experiment, the speed adaptive observer gain was used for the SMO in order to suppress the chattering problem. The saturation function and the first-order LPF were still utilized to reduce the chattering. The cut-off frequency f_c of the first order LPF were set as a constant value. However, phase delay compensation was not conducted in this experiment.

Fig. 6 shows the experimental result on the back-EMF estimation of the PMSM by using the SMO with saturation function and the speed adaptive observer gain at 40 rpm and its FFT analysis.

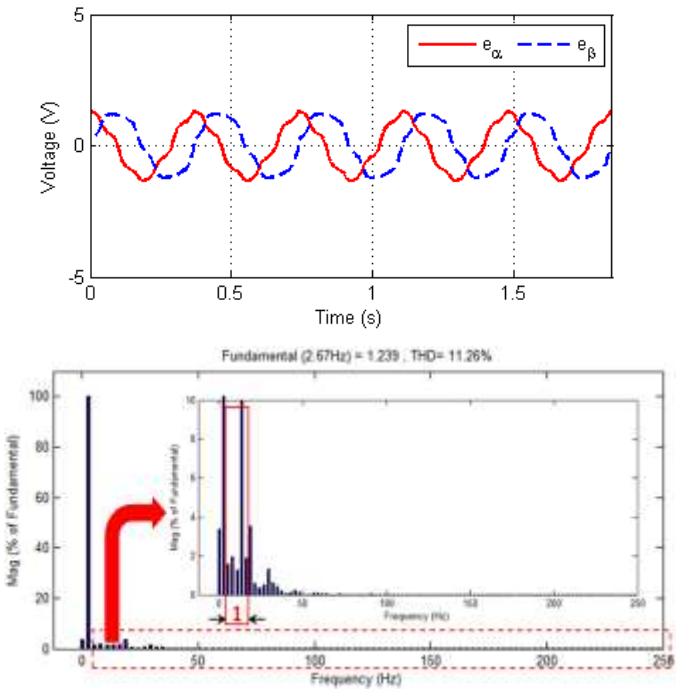

Fig. 6 Experimental result of back-EMF by using the SMO with the saturation function and the speed adaptive observer gain at 40 rpm and its FFT analysis ($f_c = 133.33Hz$). (From top to the bottom: back-EMF estimation, FFT analysis on the back-EMF)

From FFT analysis on the back-EMF shown in Fig. 6, the THD was 11.26%. The speed adaptive observer gain significantly decreased the chattering problem. Another consideration is also performed to progress estimation performance of the back-EMF in low speed area.

D. The SMO by using saturation function, cascade LPF with variable cut-off frequency (VCF), and phase delay compensation

In this experiment, the SMO was combined with saturation function and cascade LPF with variable cut-off frequency to strengthen the filtering performance. The cut-off frequency of the LPF, $f_c = nP/120$, was connected with rotating motor speed. Also, phase delay compensation was applied to overcome the big phase delay problem caused by the cascade LPF. The observer gain K was set as a constant value in this experiment.

Fig. 7 shows the experimental result on the back-EMF estimation of the PMSM by using the SMO with the saturation function, the cascade LPF with VCF, and phase delay compensation at 40 rpm and its FFT analysis. The observer gain K was set as 104.

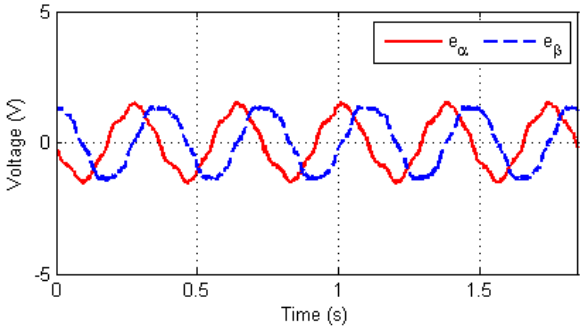

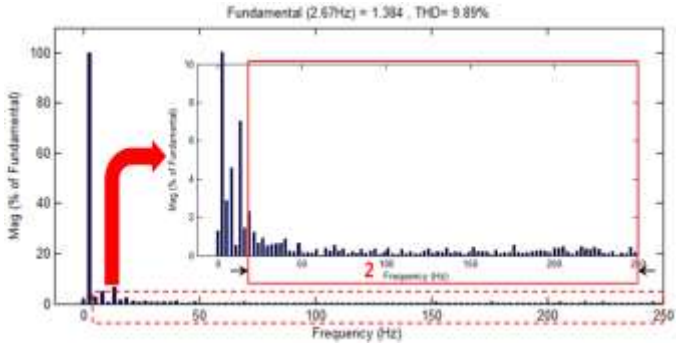

Fig. 7 Experimental result of back-EMF and its FFT analysis by using the SMO with the saturation function, the cascade LPF with VCF, and phase delay compensation at 40 rpm($K = 104$). (From top to the bottom: back-EMF estimation, FFT analysis on the back-EMF)

From FFT analysis on the back-EMF shown in Fig. 7, the THD result was 9.89%. We note here that the SMO considerably decreased the chattering problem comparing to another three cases mentioned above. Finally, the speed adaptive gain is added to this case *D* to accomplish more precise sensorless control performance in the low speed area.

E. The proposed SMO

In this experiment, the proposed SMO with saturation function was examined to clarify the effectiveness of the control performance in low speed. The speed adaptive observer gain and the cascade LPF with VCF were used to improve the sensorless vector control of the PMSM. Moreover, the phase delay compensation was also applied to overcome the big phase delay problem.

Fig. 8 shows the experimental result on the back-EMF estimation of the PMSM by using the proposed SMO at 40 rpm and its FFT analysis.

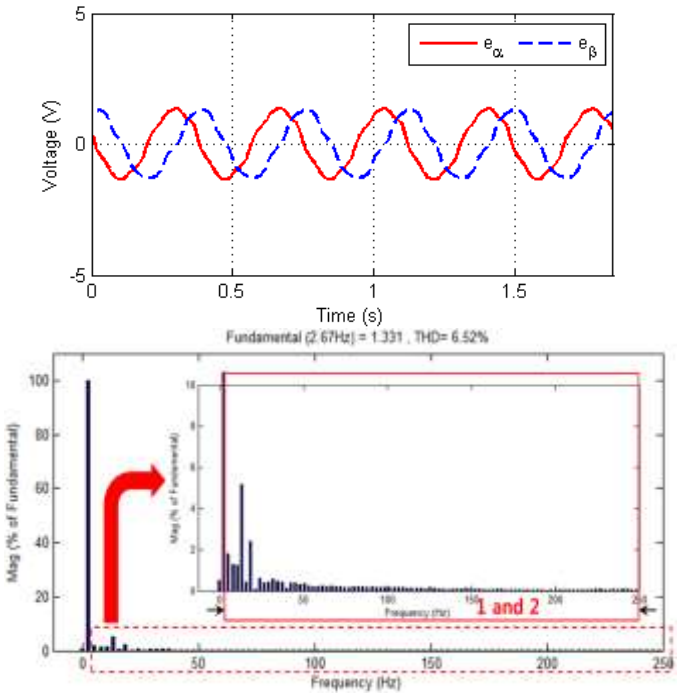

Fig. 8 Experimental results of the PMSM by using the proposed SMO at 40 rpm. (From top to the bottom: back-EMF estimation, FFT analysis on the back-EMF)

From FFT analysis on the back-EMF shown in Fig. 8, the THD result was 6.52%. The proposed SMO successfully decreased the chattering problem. Fig. 9 shows the experimental result at 10 rpm by the proposed SMO.

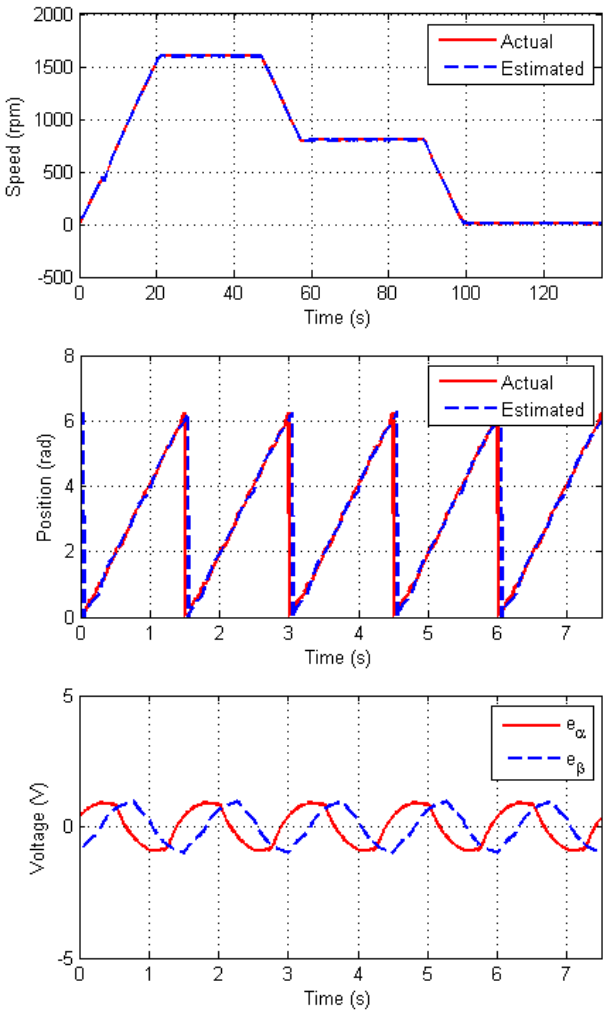

Fig. 9 Sensorless control performance of the PMSM with the proposed SMO at 10 rpm. (From top to the bottom: speed response, rotor flux position, back-EMF estimation)

From the Fig. 9, the sensorless vector control of the PMSM worked well even at 10 rpm or 0.005 p.u. from the rated value by applying the proposed SMO. The proposed SMO shows good improvement in the sensorless performance of the PMSM.

The chattering problem has been a major drawback of the conventional SMO. Some strategies were applied to the conventional SMO and analyzed the effect of the chattering suppression based on the experiment and FFT analysis.

V. Conclusions

This paper investigates strategies to improve the sensorless control performance of a PMSM with SMO for electric propulsion system of small ships. The speed adaptive observer gain, the cascade LPF with variable cut-off frequency, and phase delay compensation were utilized to escalate and to expand the speed operation range of the PMSM by the proposed SMO. The experimental results implied that the proposed sensorless control of PMSM based on the SMO have fairly good performances. Consequently, the control performance was improved particularly in the

https://doi.org/10.17758/EAP.EAP517021

low-speed operation by applying the proposed SMO.

ACKNOWLEDGMENT

This work was supported by the Technological Innovation R&D Program (C0406573) funded by the Small and Medium Business Administration(SMBA, Korea)

REFERENCES

[1] J. J. Ren, Y. C. Liu, N. Wang, and S. Y. Liu, “Sensorless control of ship propulsion interior permanent magnet synchronous motor based on a new sliding mode observer,” *ISA Trans.*, pp. 1–12, Sep 2014.
[2] A. Accetta, M. Cirrincione, and M. Pucci, “TLS EXIN based neural sensorless control of a high dynamic PMSM,” *Control Eng. Pract.*, vol. 20, no. 7, pp. 725–732, July 2012.
[3] Y. Jung and M. Kim, “Sliding Mode Observer for Sensorless Control of IPMSM Drives,” *J. Power Electron.*, vol. 9, no. 1, pp. 117–123, 2009.
[4] R. Ingale, “Harmonic Analysis Using FFT and STFT,” *Int. J. Signal Process Imange Process Pattern Recognit*, vol. 7, no. 4, pp. 345–362, 2014.
[5] Z. Qiao, T. Shi, Y. Wang, Y. Yan, C. Xia, and X. He, “New Sliding-Mode Observer for Position Sensorless Control of Permanent-Magnet Synchronous Motor,” *IEEE Trans. Ind. Electron.*, vol. 60, no. 2, pp. 710–719, 2013.
[6] H. Lee and J. Lee, “Design of Iterative Sliding Mode Observer for Sensorless PMSM Control,” *IEEE Trans Control Syst Techno*, vol. 21, no. 4, pp. 1394–1399, July 2013.
[7] D. Xu, S. Zhang, and J. Liu, “Very-Low Speed Control of PMSM Based on EKF Estimation With Closed Loop Optimized Parameters,” *ISA Trans*, vol. 52, no. 6, pp. 835–43, November 2013.
[8] J. Holtz and J. Juntao, “Sensorless Vector Control of Induction Motors at Very Low Speed Using a Nonlinear Inverter Model and Parameter Identification,” *IEEE Trans. Ind. Appl*, vol. 38, no. 4, pp. 1087–1095, July 2002.
[9] D. Raca, P. García, D. D. Reigosa, F. Briz, and R. D. Lorenz, “Carrier-Signal Selection for Sensorless Control of PM Synchronous Machines at Zero and Very Low Speeds,” *IEEE Trans. Ind. Appl*, vol. 46, no. 1, pp. 167–178, 2010.
[10] Wibowo Wahyu Kunto, and S. K. Jeong, "Improved estimation of rotor position for sensorless control of a PMSM based on a sliding mode observer," *Journal of Central South University*, vol. 23, no. 7, pp. 1643-1656, July 2016.
[11] S. M Kazraji, R. B. Soflayi, and M. B. B. Sharifian, "Sliding-mode observer for speed and position sensorless control of linear-PMSM," *Electrical Control and Communication Engineering*, vol. 5, no. 1, pp. 20-26, May 2014.
[12] H. Kim, J. Son, and J. Lee, "A high-speed sliding-mode observer for the sensorless speed control of a PMSM," *IEEE Transactions on Industrial Electronics*, vol. 58, no. 9, pp. 4069-4077, December 2010.
[13] Jiang, D., Zhao, Z., and Wang, F, "A sliding mode observer for pmsm speed and rotor position considering saliency," *Power Electronics Specialists Conference*, pp. 809-814, August 2008.
[14] A. Piippo, M. Hinkkanen, and J. Luomi, "Analysis of an adaptive observer for sensorless control of interior permanent magnet synchronous motors," *IEEE Transactions on Industrial Electronics*, vol. 55, no. 2, pp. 570-576, January 2008.
[15] N Bianchi, et al, “Comparison of PM motor structures and sensorless control techniques for zero-speed rotor position detection," *IEEE transactions on power Electronics*, vol. 22, no. 6, pp. 2466-2475, November 2007.
[16] J. H Jang, et al, "Sensorless drive of surface-mounted permanent-magnet motor by high-frequency signal injection based on magnetic saliency," *IEEE Transactions on Industry Applications*, vol. 39, no. 4, pp. 1031-1039, July 2003.
[17] J. I. Ha, et al, "Sensorless rotor position estimation of an interior permanent-magnet motor from initial states," *IEEE Transactions on Industry Applications*, vol. 39, no. 3, pp. 761-767, May 2003.
[18] S. Ostlund, and M. Brokemper. "Sensorless rotor-position detection from zero to rated speed for an integrated PM synchronous motor drive," *IEEE Transactions on Industry Applications*, vol. 32, no. 5, pp. 1158-1165, August 2002.
[19] J. C. Moreira, "Indirect sensing for rotor flux position of permanent magnet AC motors operating over a wide speed range," *IEEE Transactions on Industry Applications*, vol. 32, no. 6, pp. 1394-1401, August 1996.

Jaemin Lee is with Department of Interdisciplinary of Mechatronics Engineering, PKNU Busan, 48547, Korea (e-mail: mywoals125@ naver.com).
He is interested in the part of advanced motion control by AC motors, application of PMSM, electric propulsion system, sensorless control, and sequential control by PLC. He is trying to apply this sensorless control to hybrid propulsion system for small ships which is receiving high attention because of eco-friendly environment.

Wahyu Kunto Wibowo is with Department of Electrical Engineering, Universitas Pertamina, Jakarta, Indonesia (e-mail: wahyukuntowibowo@gmail.com).
He received his M.E. and Ph.D. in Department of Interdisciplinary of Mechatronics Engineering from PKNU in Korea. His research interests include sensorless control of PMSM, Anti-pinch control in a smart car, design of robust control system, motion control by DC and AC motors, and electric propulsion system.

Seokkwon Jeong is coauthor with Department of Refrigeration and Conditioning Engineering, PKNU, Busan, 48547, Korea (e-mail: skjeong@pknu.ac.kr).
He is a Professor Dept. of Refrigeration and Air Conditioning Engineering at PKNU. He received his M.E. and Ph.D. in Dept. of Electrical and Information Engineering from Yokohama National University in Japan. His research interests include automatic control of the refrigeration and air conditioning system, motion control using AC motors, modeling of discrete system, and electric propulsion system by AC motors.